Freehand Ultrasound Reconstruction Based on ROI Prior Modeling and Normalized Convolution

Raúl San José Estépar[1], Marcos Martín-Fernández[2], Carlos Alberola-López[2⋆], James Ellsmere[1], Ron Kikinis[1], and Carl-Fredrik Westin[1]

[1] Surgical Planning Laboratory, Harvard Medical School and Brigham and Women's Hospital, 75 Francis St., Boston, MA 02115 USA
{rjosest,jellsmere,westin}@bwh.harvard.edu
[2] E.T.S.I. Telecomunicación, University of Valladolid, Spain
{marcmar,caralb}@tel.uva.es

Abstract. 3D freehand ultrasound imaging is becoming a widespread technique in medical examinations. This imaging technique produces a set of irregularly spaced B-scans. Reconstructing a regular grid from these B-scans is a challenging problem that enables the visualization and further analysis of the acquired data. This paper focuses on extending an existing method [1] to define the output reconstruction grid based on principal component analysis (PCA). Our method introduces a model for the region of interest (ROI) in order to adapt the grid to the ROI. In addition, a technique based on normalized convolution is proposed for the interpolation problem. A new applicability function based on the correlation function of a linear probe is used to avoid inter-resolution cell blurring.

1 Introduction

Three dimensional (3D) ultrasonic imaging is increasingly being used as a diagnostic tool as well as in the operation room for surgical guidance. In freehand imaging, a 3D positioning sensor provides a measure of the position and the orientation of the coordinate system of a receiver (typically attached to the probe) with respect to a fixed coordinate system located at the transmitter. A rigid transformation allows us to convert each position in the B-scan plane to a 3D spatial position. The acquired data can be seen as a scattered distribution of planes in the 3D space. The reconstruction of a volume out of a number of planes with arbitrary orientations is still needed to apply further processing with off-the-shelf algorithms, although a real time visualization based on raw B-scans is possible and allows on-line diagnosis [2].

Volume reconstruction of ultrasounds has been tackled by several authors [3, 4,5] in the past. All these studies, despite their unobjectionable quality, share the same pitfall: no attention is paid to the details of the construction of the regular

⋆ to whom correspondence should be addressed

R.E. Ellis and T.M. Peters (Eds.): MICCAI 2003, LNCS 2879, pp. 382–390, 2003.

grid. We have recently addressed this problem [1], focusing on the three following subproblems: the selection of the coordinate system of the reconstruction grid, the selection of the extent of the reconstructed volume and the determination of the voxel size. Principal component analysis (PCA) was used in that study to deal with the first of the aforementioned subproblems. Considering the 3D positions of the pixels as samples of a population, we look for the coordinate system that achieves the largest data variance in each direction while being uncorrelated with the others. The size of the reconstructed volume is pruned using the eigenvalues information provided by PCA. We have shown [1] that this technique encloses the region of interest (ROI) with a smaller overall physical volume than other methods previously proposed in the literature.

This paper aims at extending our previous technique. A prior of the ROI is defined in order to weight the PCA stage. The ROI prior is defined as two independent distributions in both the axial and lateral directions. The model parameters are estimated in a maximum likelihood sense from a few ROI delineations. Moreover, we propose the use of normalized convolution [6] to perform the interpolation of the irregular sampled data. The proposed normalized convolution method takes into account the point spread function of the aperture. Thus, the interpolation scheme is tuned to the resolution cell of the ultrasound system, avoiding a inter-resolution cell blurring.

2 Methods

2.1 Coordinate System Extraction

In this work, we introduce an enhancement of the method proposed in [1] by including a ROI prior in the PCA computation. The coordinate system associated with the output grid is computed from an principal component analysis of the data points (B-scan pixels) positions. The covariance matrix of the positions defines the transformation between the transmitter coordinate system and the output grid coordinate system (see Fig. 1a).

A prior defines the probability for a given point in the B-scan plane to belong to the ROI. We propose a prior probability density function (pdf) that follows a Gaussian distribution in the lateral direction and a Rayleigh distribution in the axial direction.

$$p(s,q;\theta_{s1},\theta_{s2},\theta_{q1}) = p_{lat}(s)p_{ax}(q) = \frac{1}{\theta_{s2}\sqrt{2\pi}} e^{-\frac{(s-\theta_{s1})^2}{2\theta_{s2}^2}} \frac{q}{\theta_{q1}^2} e^{-\frac{q^2}{2\theta_{q1}^2}}. \quad (1)$$

The further in the axial direction the more unlikely to find a point that, a priori, belongs to the ROI due the fact that the ultrasound signal undergoes an in-depth attenuation that makes preferable to localize the object of interest near the focus. In that sense, a Rayleigh distribution accounts quite well for that behavior. The prior parameters can be estimated by a maximum likelihood approach. Let us assume that we are able to know the points that belong to the ROI along some slices in our study, $\mathbf{S} = \{s_i\}$ and $\mathbf{Q} = \{q_i\}$, where $i = 1 \ldots N$. The log-likelihood

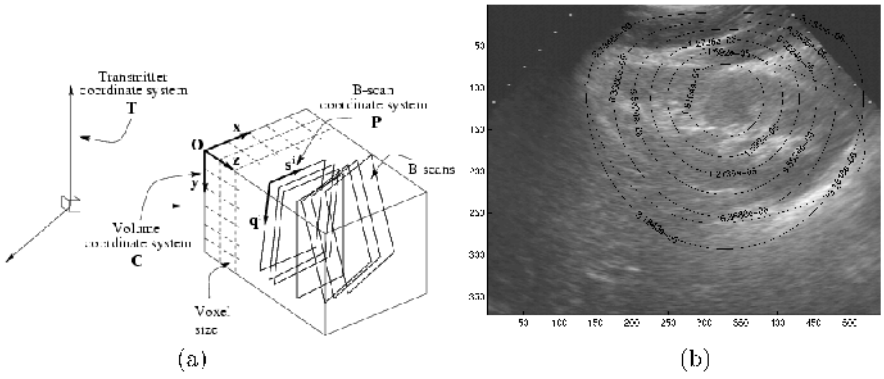

Fig. 1. (a) Coordinate systems involved in the grid definition.(b) Prior distribution contour plot on a kidney examination

function is given by $\mathcal{L}(\theta|(\mathbf{S},\mathbf{Q})) = \log \prod_{i=1}^{N} p_{lat}(s_i|(\theta_{s1},\theta_{s2}))p_{ax}(q_i|\theta_{q1})$. The parameters that maximize this function can be easily worked out, resulting on

$$\theta_{s1} = \frac{1}{N}\sum_{i=1}^{N} s_i \qquad \theta_{s2} = \frac{1}{N}\sum_{i=1}^{N}(s_i - \theta_{s1})^2 \qquad \theta_{q1} = \sqrt{\frac{\sum_{i=1}^{N} q_i^2}{2N}}. \tag{2}$$

Figure 1b shows the prior distribution contour plot overlaid with the corresponding B-scan of a kidney examination. The ROI has been delineated (dashed contour) and eq. (2) have been used to compute the prior parameters.

The prior pdf is used to weight the position of each pixel in the covariance matrix estimation. The eigenvectors of the covariance matrix define the output coordinate axis. The eigenvalues are used to compute the extent of the output grid allowing a trimming as reported by [1]. The length of the trimmed output grid along coordinate i that confines a given information density, say r, is $l_i = 2\sqrt{2\lambda_i} \cdot erfinv\left(r^{1/3}\right)$, where λ_i is the eigenvalue for coordinate i and $erfinv$ is the inverse error function.

2.2 Regular Sampling from Sparse Data

The signal reconstruction from irregularly sparse sampled data is the main problem to overcome in freehand imaging once the coordinate system problem has been resolved. Solutions that primely favor the simplicity and performance, i.e. nearest neighbor solutions, have prevailed in the literature, for example [7].

We attempt to provide a localized solution while preserving computational resources by means of spatial locality. This solution is based on normalized convolution [6] to filter uncertain and sparsely sampled data. Normalized convolution can be seen as a local weighted least square solution where the weights are given by two terms: an certainty function, c, and an applicability function, a.

The former encompasses the knowledge of our data being missing. The applicability function tries to enforce locality to the solution by giving less importance to samples further away the location of your output sample. In the case of using a constant basis function, the normalized convolution expression reduces to $\tilde{f} = \frac{\sum_j a(\mathbf{x}_j)c_j f_j}{\sum_j a(\mathbf{x}_j)c_j}$. We will not elaborate further on normalized convolution but refer the interested reader to the seminal references [6].

The ultrasound reconstruction problem has being traditionally divided in two parts: bin filling and hole filling. The former accounts for resolving a single value on the grid locations where several input samples contribute. The latter estimates the values of the remaining output grid positions. A theoretical distinction between bin and hole filling allows to build a certainty function that behaves differently when dealing with subvoxel interpolation and intervoxel interpolation.

Certainty function. In this work, the local certainty function consists of two part to account for the bin filling and hole filling process:

1. A *bin* measure, c_b, defined in the input data. This measure decides what to do when several pixels lie into the same voxel. Operations like averaging, median or maximum value could be implemented by properly setting c_b.
2. A *hole* measure, c_h, defined in the output grid. This function tells the locations where no data exist.

Applicability function. It has been specially designed to account for the asymmetric shape of the point spread function of the ultrasound beam. The point spread function determines the resolution cell of our system. Our applicability function should take this into account to avoid blurring beyond the system resolution; therefore, the output structural blurring is minimize making the interpolation process as local as possible to the information that lies into the resolution cell.

The applicability function proposed in this paper is given by three terms: $a(s,q,t) = R_{ax}(q)R_{la}(s)R_{el}(t)$, where R stems from the correlation functions of a rectangular aperture that can be analytically resolved [8]:

$$R_{la}(s) = \frac{1}{(\pi s)^2}\left[1 - \frac{sin(2\pi f_s s)}{2\pi f_s s})\right], \qquad R_{ax}(q) = e^{-\frac{q^2}{4\sigma_q^2}}, \qquad R_{el}(t) = e^{-\frac{t^2}{4\sigma_t^2}}. \tag{3}$$

In a far field approximation every aperture can be seen as a rectangular one, making eq. (3) feasible. The parameters f_q, σ_s and σ_t have a physical meaning associated with probe parameters: $f_s = \frac{D}{\lambda_0 s_0}$, $\sigma_q^2 = \frac{\lambda_0^2}{16 \ln 2}$ and $\sigma_t^2 = \frac{\lambda_0^2}{4}$. λ_0 is the transducer wavelength, D is the aperture width and s_0 is the focal depth.

3 Results

Coordinate system evaluation. The evaluation has been carried out using a thyroid and a kidney examination. An expert was requested to scroll along the

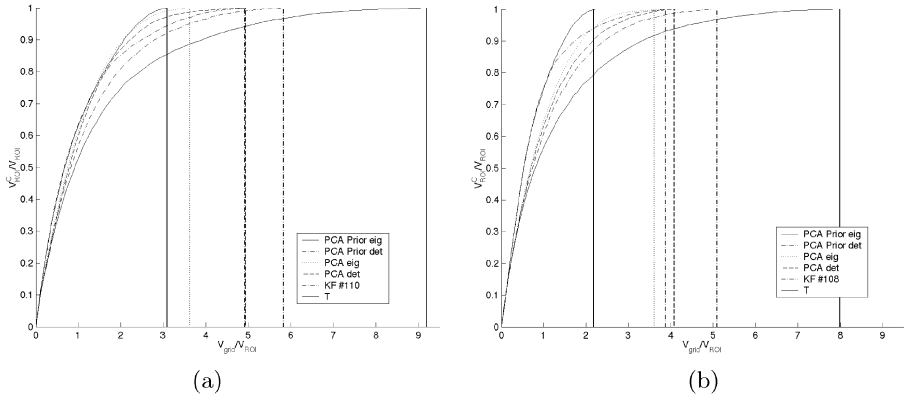

(a) (b)

Fig. 2. Evolution of the V^c_{ROI} with V_{grid}, both normalized by V_{ROI}. Two cases have been analyzed: (a) thyroid gland and (b) kidney. Vertical lines show the point at which each method starts to enclose the ROI.

volumes and delineate the ROI in a set of representative slices. This initial delineation was used to estimate the prior pdf parameters using eq. (2). Later on, the same expert was requested to carefully delineate the ROI along the whole examination, so a quantitative study could be conducted.

The proposed coordinate system has been compared with other three methods: PCA without using ROI prior, Key-frame and the transmitter coordinate system (hereon referred as the T method). Key-frame merely sets up the coordinate system by choosing one of the study B-scan coordinates as grid coordinate system. The transmitter coordinate system is the one given directly for the tracking system (see Fig. 1a). For the PCA systems two trimming methods has been used: the proposed eigenvalues approach and a deterministic approach based on the deviation from the center of gravity and an external percentage p [1]. Key-frame and T methods have been solely trimmed with the deterministic method due the lack of eigenvalues in those cases. We evaluate the coordinate system by analyzing the ROI volume encompassed for the grid as the trimming method includes more and more information. ROC-like curves are shown in which the magnitude in the horizontal axis is the physical volume of the reconstructed grid (V_{grid}), and the magnitude in the vertical axis is the portion of the ROI captured by the reconstructed grid (V^c_{ROI}). Both axis are normalized by the physical volume of the ROI (V_{ROI}) in order for the curves of the two datasets to be comparable irrespective of the actual size of the ROI.

Figure 2 shows the Receiver Operating Characteristic (ROC) curves that result from the different methods for the two studies. The ROI method significantly improves the results, overall when the eigenvalues are used to trim the volume. We have observed that the ROI prior greatly enhance the information carried by the eigenvalues of the covariance matrix. We have also seen that the trimming method is less sensitive to the variation of r when the ROI prior is

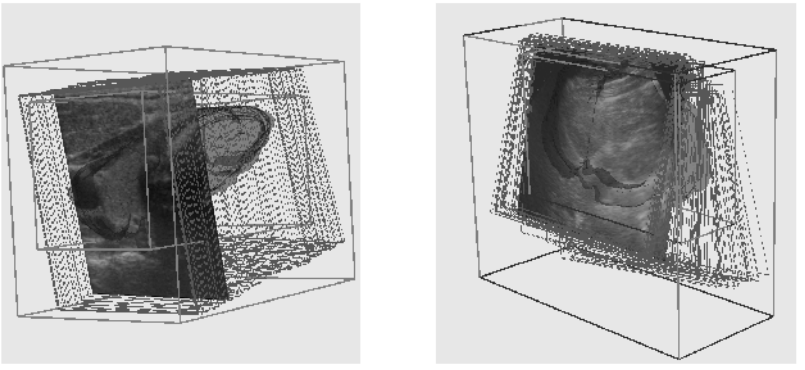

Fig. 3. Performance of the ROI prior method with the eigenvalue trimming approach. The original B-scans planes, the bounding box (outer box) and box for $r = 0.8$ are shown for the cases (a) thyroid gland and (b) kidney.

taken into account. Figure 3 shows the output grids when the PCA with ROI prior is applied. r has been set to 0.8. A ROI model has been rendered to let the reader assess the goodness of the result. The outermost box is the bounding box that covers the whole data for the PCA coordinate system.

Normalized convolution. The interpolation has been assessed using two studies. First, an examination of a thyroid gland performed with a 7 MHz linear array probe and a depth setting of 40 mm depth. The second examination was performed with a 6.5 MHz laparoscopic convex curvilinear array probe and a depth setting of 35 mm. The performance of the proposed applicability function using normalized convolution (NC) has been compared with other three interpolation methods. A simple nearest neighbor approach (NN), a inverse distance-weighted approach (DW) and a triangle-based interpolation (TgLinear) [9] using the Matlab *griddata* implementation.

Since an underlying anatomical ground truth is not known, we have decided to test our method by artificially removing data from the two examinations. For a given slice, the voxel array has been aligned with this B-scan such that pixels fall exactly onto voxels. Pixels of this B-scan have been randomly removed from a uniform distribution. The corresponding interpolation algorithm has been applied over this artificial irregular sampled slab. The tests have been carried out along 6 different B-scans for both volumes. For each B-scan, ten different percentages of data have been removed: 5% and from 10% to 90% in 10% increments. For each percentage, the test has been repeated ten times such that new random pixels are drawn each time. The root mean squared error (RMS) between the interpolated and the original data has been computed as performace measure.

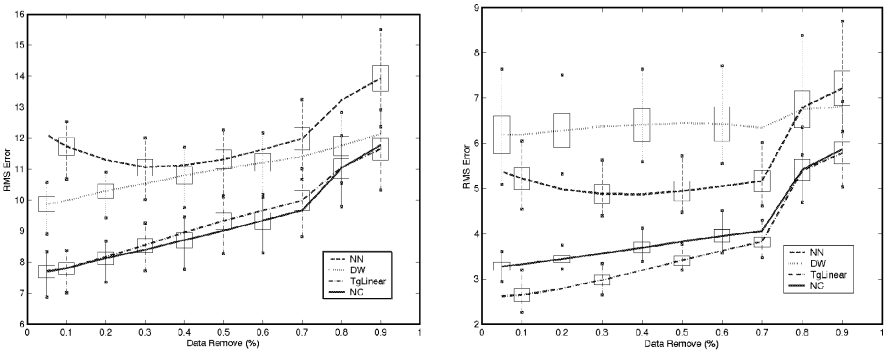

Fig. 4. Evaluation of the interpolation method.(a) Thyroid case.(b) Pig hepatic vein case. Mean RMS error is plotted with lines, the standard deviation with boxes and the outliers values at the end of the whiskers.

Figure 4 shows the overall trend of the methods under analysis. Our method performs as well as TgLinear. However, our method is on average four times faster. Moreover, TgLinear is not feasible when the number of fitting points become larger and lager. In our case, we are not limited by this factor. Figure 5 illustrate a set of interpolated images when 60% of the data is removed. In general, NC shows a good signal recovery without structural blurring. These visual results validate the way that the applicability function has been built. Methods like NN and TgLinear show a result that looks more alike the original, although artifact are introduced in the structures, as it can be seen.

4 Conclusions

A reconstruction method for freehand ultrasound has been presented. The main contribution has been an extension of an PCA-based approach to find out the optimum coordinate system. This extension is based on fitting a prior model for the ROI in order to get the best grid that encloses the ROI. Moreove, we has proposed a new applicability function that takes into account the physical characteristic of the probe in order to localize the interpolation problem to the system resolution in a normalized convolution framework. Our method seems to outperform existing methods both numerically and visually.

Acknowledgements. The first author would like to thank Anders Brun for his useful comments reviewing this paper. This work was partially funded by NIH grant P41-RR13218 and by CIMIT.

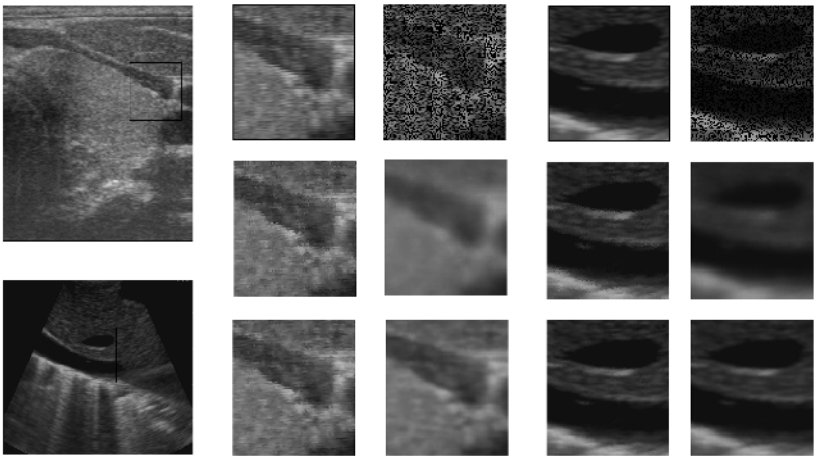

Fig. 5. Interpolation results. (a) Original slices: a thyroid (top), a hepatic vein of a pig (bottom). Details for the thyroid case (b) and pig hepatic vein (c). From top to bottom, left to right: original, missing data, NN, DW, TgLinear and NC.

References

1. Raúl San José Estépar, Marcos Martín-Fernández, P. Pablo Caballero-Martínez, Carlos Alberola-López, and Juan Ruiz-Alzola. A theoretical framework to three-dimensional ultrasound reconstruction from irregularly-sampled data. *Ultrasound in Medicine & Biology*, 29(2):255–269, 2003.
2. Richard W. Prager, Andrew Gee, and Laurence Berman. Stradx: real-time acquisition and visualization of freehand three-dimensional ultrasound. *Medical Image Analysis*, 3(2):129–140, June 1999.
3. C. D. Barry, C. P. Allott, N. W. John, P. M. Mellor, P. A. Arundel, D. S. Thomson, and J. C. Waterton. Three-dimensional freehand ultrasound: image reconstruction and volume analysis. *Ultrasound in Medicine & Biology*, 23(8):1209–1224, 1997.
4. Robert N. Rohling, Andrew H. Gee, and Laurence Berman. Three-dimensional spatial compounding of ultrasound images. *Medical Image Analysis*, 1(3):177–193, 1997.
5. Stephen Meairs, Jens Beyer, and Michael Hennerici. Reconstruction and visualization of irregularly sampled three- and four-dimensional ultrasound data for cerebrovascular applications. *Ultrasound in Medicine & Biology*, 26(2):263–272, 2000.
6. H Knutsson and C.-F. Westin. Normalized and differential convolution: Methods for interpolation and filtering of incomplete and uncertain data. In *Proc. of IEEE Computer Society Conference on Computer Vision and Pattern Recognition*, pages 515–523, 1993.
7. T. R. Nelson and D. H. Pretorius. Interative acquisition, analysis and visualization of sonographic volume data. *International Journal of Imaging Systems and Technology*, 8:26–37, 1997.

8. R. F. Wagner, S. W. Smith, J. M. Sandrik, and H. Lopez. Statistics of speckle in ultrasound b-scans. *IEEE Trans. on Sonics and Ultrasonics*, 30(3):156–163, May 1983.
9. David F. Watson. *Contouring: A guide to the analysis and display of spacial data.* Pergamon, 1994.